Preprint typeset in JINST style - HYPER VERSION

The brighter-fatter effect and pixel correlations in CCD sensors

P. Antilogus[a], P. Astier[a]*, P. Doherty[b], A. Guyonnet[a] and N. Regnault[a]

[a] *LPNHE/IN2P3/CNRS,*
UPMC, 4 place Jussieu F75005 Paris, France
[b] *Department of Physics, Harvard University,*
17 Oxford Street, Cambridge, MA 02138, USA
E-mail: pierre.astier@in2p3.fr

arXiv:1402.0725v1 [astro-ph.IM] 4 Feb 2014

ABSTRACT: We present evidence that spots imaged using astronomical CCDs do not exactly scale with flux: bright spots tend to be broader than faint ones, using the same illumination pattern. We measure that the linear size of spots or stars, of typical size 3 to 4 pixels FWHM, increase linearly with their flux by up to 2 % over the full CCD dynamic range. This brighter-fatter effect affects both deep-depleted and thinned CCD sensors. We propose that this effect is a direct consequence of the distortions of the drift electric field sourced by charges accumulated within the CCD during the exposure and experienced by forthcoming light-induced charges in the same exposure. The pixel boundaries then become slightly dynamical: overfilled pixels become increasingly smaller than their neighbors, so that bright star sizes, measured in number of pixels, appear larger than those of faint stars. This interpretation of the brighter-fatter effect implies that pixels in flat-fields should exhibit statistical correlations, sourced by Poisson fluctuations, that we indeed directly detect. We propose to use the measured correlations in flat-fields to derive how pixel boundaries shift under the influence of a given charge pattern, which allows us in turn to predict how star shapes evolve with flux. We show that, within the precision of our tests, we are able to quantitatively relate the correlations of flat-field pixels and the broadening of stars with flux. This physical model of the brighter-fatter effect also explains the commonly observed phenomenon that the spatial variance of CCD flat-fields increases less rapidly than their average.

KEYWORDS: Detectors for UV, visible and IR photons (solid-state); Image processing.

*Corresponding author.

Contents

1. Introduction **1**

2. Detecting the brighter-fatter effect **2**

3. PTC non-linearity and statistical correlations in flat-fields **4**

4. Coulomb forces in CCDs **5**
4.1 Simplified calculations from first principles 5
4.2 A generic model for electrostatic distortions of drift fields 7

5. Closing the loop: deriving the brighter-fatter slope from flat-field correlations **10**
5.1 Solving for the model coefficients from flat-fields 10
5.2 Comparing predicted and measured brighter-fatter slopes 10

6. Discussion **12**

1. Introduction

The astronomical use of CCDs very commonly assumes that these sensors slice the incoming light along a regular lattice of pixels, each of which then responds independently of what adjacent pixels receive. Non-linearity usually refers to the reponse of the electronic chain, which can be (and often is) corrected independently for each pixel.

In this representation, the images scale precisely with the incoming flux or staring time on a static scene, possibly after some linearity restoration is applied at the pixel level. We will discuss in this contribution a tiny violation of this idealistic picture of CCDs: images of stars (or laboratory spots) do not exactly scale with the incoming flux, even with a prefectly linear readout chain. With increasing flux, images of spots or stars tend to broaden: the measured sizes grow linearly with flux. Since the effect is almost isotropic (though not exactly), there is a strong inclination to attribute it to sensors rather than to the read out chain. All attempts to detect the effect we know about have been successful, and the effect does not seem to only affect deep-depleted CCDs.

There is another known departure from the independent pixels representation: the variance of a flat-field image does not grow linearly with the exposure average (as Poisson statistics robustly predict), but the variance "flattens out", as if some mechanism washing the contrast were at play. This phenomenon is sufficiently similar to the brighter-fatter effect to attempt to bridge these two effects.

The flattening of the photon transfer curve (PTC i.e. the spatial variance of flat-fields as a function of their average) is known to be reduced or to almost disappear by summing neighboring

pixels into larger pixels (e.g. [1]). This indicates that the variance of a sum of neighboring pixels is larger than the sum of their variances, and adjacent pixels should therefore have (positive) covariances. We detect these covariances. They contain more information than the flattening of the PTC, and we will hence study pixel correlations in flat-field images rather than the "missing variance" one can extract from the shape of the PTC.

Large scale imaging surveys, underway and anticipated, vitally require precise knowledge of their Point Spread Function (PSF). Regarding the accuracy of the PSF shape and size, the most demanding application is arguably the measurement of the shear of background galaxy images induced by mass density gradients along the line of sight, in order to constrain these mass gradients, and in turn cosmology. Usually, the design of the data reduction chain assumes that stars collected in the science image are faithful models of the PSF, so that the effects of the observing system (possibly including atmosphere) on objects shapes can be measured and "factored out" using these stars. We will argue that stars are acceptable PSF templates only for applications that can accommodate an inaccuracy of the PSF size at the percent scale. In particular, studying the correlations of the shear field measured from galaxy shapes now requires a PSF typically understood at the 10^{-3} level or better (see e.g. the contribution of M. Jarvis at this workshop[1]). The requirements on PSF ellipticity accuracy are as low as $2\ 10^{-4}$ for the Euclid space mission [2].

We attempt in this contribution to bridge the brighter-fatter effect and the correlations in flat-fields, assuming that both are a consequence of alterations of drift lines in the CCD bulk induced by charges accumulating in the potential wells of the sensor during the exposure. These drift field alterations can be regarded as dynamical modifications of pixel boundaries[2]. We wish to set up this bridge in order to derive the details of the brighter-fatter effect from pixel correlations in flat-fields. This would allow one to account for the brighter-fatter effect in the data reduction procedures, for a variety of image qualities and PSF shapes, and beyond the growth of second moments.

In this paper we proceed as follows. First we expose the characteristics of the brighter-fatter effect (§ 2). We then discuss statistical pixel correlations in flat-fields (§ 3). We propose in § 4 that Coulomb forces sourced by already collected charges on drifting ones are the source of both effects, and propose a parametrized model that explains both. In § 5, we derive the model parameters from flat-field images and then predict the brighter-fatter slope for three different sensor types. We summarize and discuss possible further work in § 6.

2. Detecting the brighter-fatter effect

It is in fact fairly easy to detect the "brighter-fatter" effect. One either needs a set of images of a spot of increasing integrated flux (in the lab, that can be done by varying the open shutter time), or an astronomical image with the full range of star brightnesses. One then measures the second moments of spots or stars using an estimator whose bias does not vary with S/N (e.g. eq. 1 from [3]). One can then observe that the linear sizes of spots increase linearly with flux, in both directions. We have detected the effect in the laboratory using spots projected on an E2V CCD250, a candidate

[1]The presentations at this workshop can be found on http://www.bnl.gov/cosmo2013/

[2]The "tree-rings" phenomenon (see the contributions of e.g. G. Bernstein, E. Magnier & R. Lupton at this workshop) is probably due to a similar phenomenon, but induced by a static distortion of the drift field sourced by spatial and static variations of the silicon bulk resistivity.

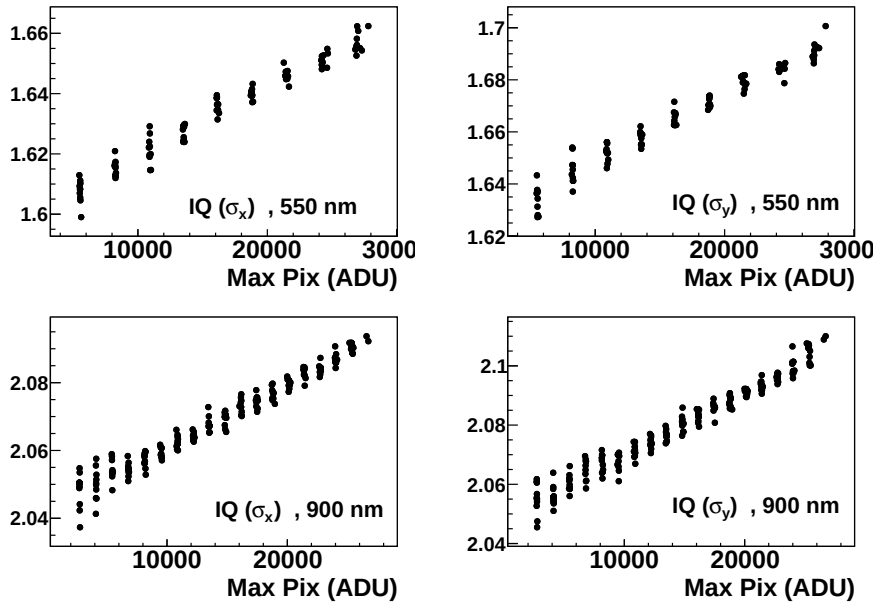

Figure 1. Measured sizes (pixels rms) of a laboratory spot along x and y coordinates of the E2V CCD250, as a function of the spot peak flux in ADUs (the gain is about 5 e-/DN). The relative increase of size is more than 2% over the full dynamic range, and slightly larger along *y* direction (parallel transfers) than along *x* (serial transfers). The relative size increases are similar at two different wavelengths. Diffraction in the illumination system is likely causing the difference in size of the spots at these two wavelengths.

sensor for the Large Synoptic Survey Telescope (LSST) camera. Our measurements, displayed in fig. 1 show that the size of the spots rises linearly with their peak flux, in both directions. The size increase amounts to 2 to 3 % at 150 ke. We have also detected the effect in on-sky data from the thinned sensors of Megacam on CFHT (type 42-90 from E2V), where it amounts to 0.5% over the full dynamic range (saturation occurs at 100 ke) and in data from DECam on the CTIO Blanco Telescope (using the publicly available science verification data), where it amounts to 1.5%. DECam is populated with CCDs manufactured by LBNL, which are deep-depleted 250 μm thick sensors. We hence measure variations of size in the % range, and consistently slightly steeper (typically 20 %) along *y* (parallel shifts), than along *x* (serial shifts). At this workshop, the effect was also reported by R. Lupton about the Hamamatsu sensors S10892-02 populating the Hyper Suprime Cam focal plane. We do not know of any sensor that does not exhibit the effect. For images from the sky, one must take care to isolate the "color independent" brighter-fatter effect from the more trivial spectral dependence of the PSF coupled to statistical relations between color and brightness in the star sample used for the measurement. We display our measurements in fig 1.

One can think of at least two applications that require knowledge of the PSF size at the % level or better: correlations of the gravitational shear over large areas on the sky, and accurate PSF photometry, in particular when measuring supernova light curves for estimating their distance. The brighter-fatter effect is a manifestation of a more general departure of star images from the actual PSF, and some handling of the effect beyond the size of the PSF should be devised. Ground-based applications face one extra complication : the slope of the effect depends of the image quality

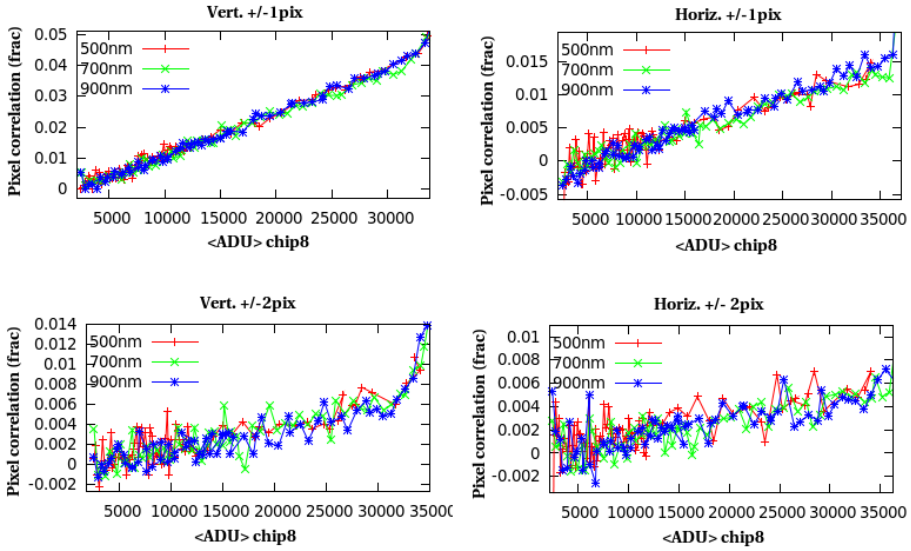

Figure 2. Correlation coefficients of flat-field pixel pairs as a function of illumination of the flat-field, at three different wavelengths. These correlations rise linearly with illumination and are achromatic. They decay with distance, and are larger along y (CCD columns) than along x, especially for the nearest neighbors. These correlations are indeed measured on differences of flat-field exposures with the same average. These measurements were carried out on the E2V CCD250 sensor, candidate for LSST.

itself, which potentially changes at every exposure. A physical understanding of the origin of the effect would then allow one to extract an unbiased PSF model from stars observed in virtually all observing conditions.

3. PTC non-linearity and statistical correlations in flat-fields

There exists one other known departure from the picture of independent pixels: the spatial variance of flat-fields is not exactly proportional to the average illumination in the flat-field, but "flattens out": high-illumination flat-fields exhibit a lower variance than would be expected from extrapolating measured variances at lower illumination. This apparent violation of Poisson statistics tends to vanish when one groups neighboring pixels into larger pixels [1]. This strongly suggests that neighboring pixels of flat-fields have statistical correlations, which we indeed found. As shown in figure 2, the correlation coefficients between nearby pixels appear to be a linear function of illumination, up to saturation, and decay rapidly with separation. They look roughly isotropic, except for the nearest neighbors where the vertical correlations seems constantly larger than the horizontal correlation (as shown as well by R. Lupton for HSC at this workshop). These correlations also look mostly achromatic.

The fact that the correlation coefficients rise linearly with the flat-field average implies that covariances rise quadratically with illumination and hence that the PTC should exhibit a (small) quadratic correction to Poisson statistics. For the E2V CCD250 we find that the size of the measured covariances fully explains the "missing variance" on the PTC.

The correlations depend on electrostatics in the CCD: lowering the clock voltages applied during collection increases the correlations in the vertical (y) direction (fig. 3). This fact, along

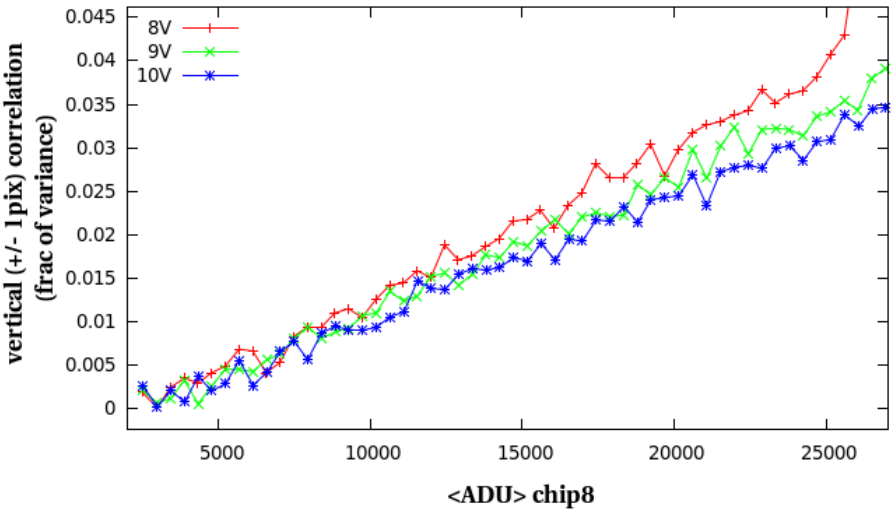

Figure 3. Same plot as figure 2, at 700nm, but for different clock voltages during collection. This indicates that correlations are likely related to electrostatics.

with an almost isotropic correlation pattern beyond first neighbors, strongly suggests that the origin of the correlations lies in the sensor itself.

4. Coulomb forces in CCDs

.

As already presented, we argue that forces produced by stored charges and experienced by subsequently collected charges are the common cause of both the brighter-fatter effect and the pixel correlations in flat-fields. We first present numerical electrostatic calculations from first principles, that show that the observed size of both effects is compatible with reasonable values of the key parameters. The reach of these simulations is however limited by our restricted knowledge of several parameters that determine the electrostatics of CCDs. We hence develop a parametrized model of drift field alterations that aims at describing both phenomena using the same algebra.

4.1 Simplified calculations from first principles

We have conducted a simplistic 3D electrostatic simulation of a CCD in order to evaluate drift lines and how they are altered when charges are present in the CCD. Our aim is not to reproduce in all details the measurements, but to assess if the size and other characteristics of the observed effects (both the brighter-fatter effect the pixel correlations) can be reproduced by the same calculation. We have simulated the E2V CCD250 geometry, i.e. 100 μm thick square pixels 10 μm on a side, in n-type silicon. We have approximated the intrinsic silicon as free of charges, and we have implemented the split across columns using the same potential pattern than the one that defines rows: our simulation clearly does not aim for a high fidelity. Given the applied voltages, we have then solved numerically for the potential, and computed drift trajectories. In particular, we have located the pixel boundaries by tracking positive charges backwards from pixel separations on the charge collecting face. Using the image series technique (see e.g. [4]), we have computed the

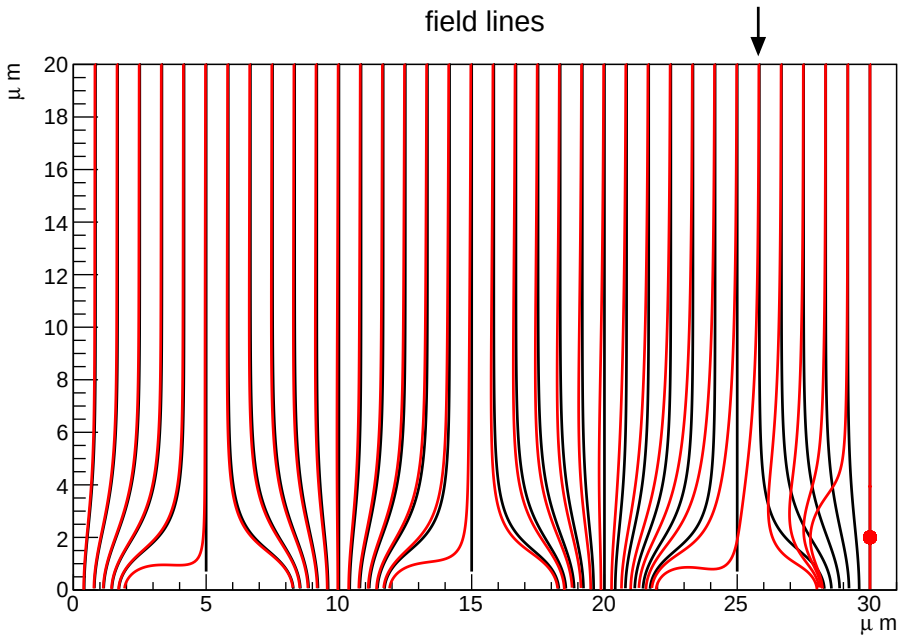

Figure 4. Computation of field lines for the E2V CCD 250 geometry, with (red) and without (black) a 50 ke charge positionned at the bottom right (red spot). An electron drifting along the arrow drawn at the top of the picture goes either left or right depending on the presence of the charge, which illustrates that the rightmost pixel shrinks when storing more charge than its neighbor. The stored charge also shifts farther pixel boundaries. Note that we have only drawn the CCD collection area, and the total device thickness is 100 μm rather than the bottom 20 μm drawn on the vertical axis.

potential of a charge between equipotential planes and added it to the potential created by the voltages applied to the sensor. We can then evaluate how drift lines are altered when some charge is stored in the CCD. We illustrate in figure 4 how some charge added in the CCD alters drift lines. From these alterations, we can derive both the brighter-fatter effect and pixel correlations in flat-fields.

Our crude simulation only has one adjustable parameter: the distance between the gate plane (which has imposed potentials) and the charge stored in a pixel. This distance is often referred to as the depth of the buried channel. We have found a fair match between our simulations and the data from the E2V CCD250 for a distance of 2.5 μm. The comparison of anticipated and measured effects is displayed in figure 5. The fact that the same simulated setup can reproduce the observed slope of the brighter-fatter effect *and* the observed scale of correlations constitutes an encouraging indication that Coulomb forces are the possible common and dominant cause of both effects.

From these simulations, we were able to evaluate that the alterations of drift trajectories mostly happen in the last microns above the clock stripes (see fig. 4), for a variety of geometries and voltage values. Because this very last part of the electron drift is experienced by all electrons, irrespective of the photon conversion depth, this Coulomb force ansatz naturally explains the observed achromaticity of correlations.

Note that when comparing electrostatic simulations to real data, one has to account for the fact that real images depict the final state of the charge distribution in the CCD, but the collection

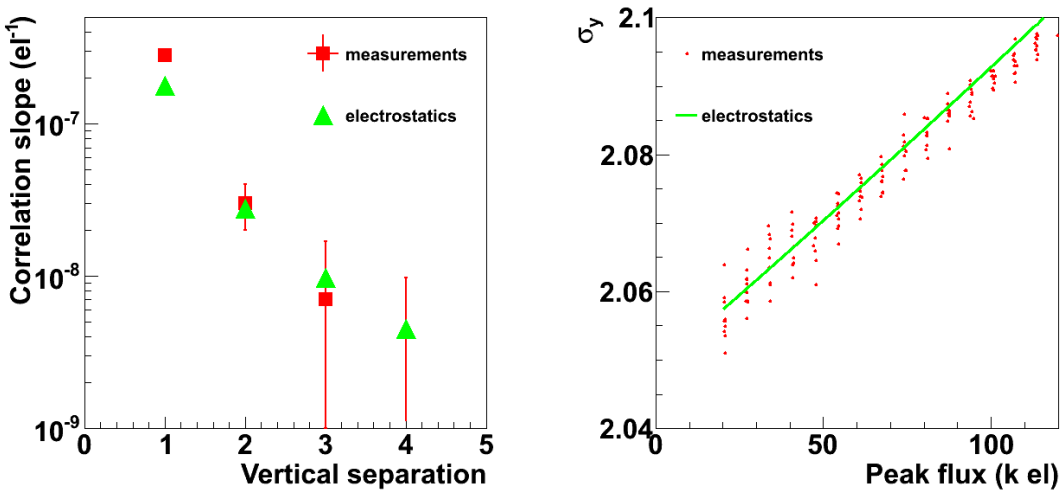

Figure 5. Comparison of our crude electrostatic simulation and measurements for the correlations along y (left) and the brighter-fatter slope (right). This indicates that Coulomb forces in CCDs have the right scale for causing both effects.

of electrons happened under less contrasted conditions, because less charge was residing at the bottom of the CCD during most of the exposure than at its end. It is fairly easy to account for this effect: on average, the charge contrasts during the exposure are half of what they are at the end, and to first order, the perturbations to pixel boundaries are proportional to the charge contrasts. So, when computing perturbations from an electrostatic simulation, one just has to halve the effects computed for the image "final state".

Making the electrostatic simulation of CCDs more and more realistic might seem a possible avenue to account for the brighter-fatter effect. However, the outcome of the fabrication process is not necessarily known precisely enough, and CCD vendors might regard some key design features as proprietary. We could then consider using the correlations in flat-fields to predict or at least constrain the brighter-fatter effect. We have then developed a generic model in order to describe both effects using the same algebra.

4.2 A generic model for electrostatic distortions of drift fields

In this section, we approximate the electrostatic influence of charges in the CCD as pixel boundary shifts. We model the displacement of the effective boundaries of a pixel, labeled $(0,0)$, caused by a charge $q_{i,j}$ in the potential well of a pixel at position (i,j) as:

$$\delta^X_{i,j} = q_{i,j} a^X_{i,j} \tag{4.1}$$

where we have expressed that the (perturbating) electric field due to a charge is proportional to this charge (which is exact), and we have approximated alterations to drift trajectories as first order perturbations. X indexes the four boundaries of the pixel $(0,0)$, and we label each boundary by the coordinates of the pixel that shares it with (0,0): $X \in \{(0,1),(1,0),(0,-1),(-1,0)\}$. The $a^X_{i,j}$

coefficients satisfy symmetries:

$$a^X_{i,j} = a^{-X}_{-i,-j} \qquad \text{(parity)} \tag{4.2}$$

$$a^{0,1}_{i,j} = -a^{0,-1}_{i,j-1} \qquad \text{(translation invariance)} \tag{4.3}$$

The $a^X_{i,j}$ also obey a sum rule:

$$\sum_{i,j} a^X_{i,j} = 0, \forall X \tag{4.4}$$

because the electric field induced on a pixel boundary (and hence the displacement of the latter) is null if all charges $q_{i,j}$ are equal. Each boundary of the pixel $(0,0)$ shifts under the influence of all charges. Because electric fields add up, the displacement reads:

$$\delta^X = \sum_{i,j} \delta^X_{i,j} = \sum_{i,j} q_{i,j} a^X_{i,j}$$

We call charge transfer the difference between charge contents with and without the perturbating electric fields. The displacement of the pixel boundary δ^X induces a charge transfer between the pixel $(0,0)$ and the pixel X, where $X \in \{(0,1),(1,0),(0,-1),(-1,0)\}$. To first order, this charge transfer is proportional to both the pixel boundary displacement and to the charge density flowing on this boundary. For a well sampled image (i.e. the charge distribution impinging on a pixel does not vary rapidly within this pixel), we can approximate the charge density drifting on the boundary between pixel $(0,0)$ and its neighbor X as:

$$\rho^X_{00} \propto (Q_{0,0} + Q_X)/2$$

so that the net charge transfer due to perturbating electric fields between pixel $(0,0)$ and its neighbor X reads:

$$\delta Q^X_{0,0} = \sum_{i,j} a^X_{i,j} Q_{i,j} (Q_{0,0} + Q_X) \tag{4.5}$$

The expression is non-linear with respect to the charge distribution: the charges $Q_{i,j}$ are the source charges, and the expression $(Q_{0,0} + Q_X)$ approximates the test charges. We have deliberately incorporated all proportionality coefficients into the $a^X_{i,j}$ factors. The perturbed charge in pixel $(0,0)$ reads:

$$Q'_{0,0} = Q_{0,0} + \delta Q_{0,0} \tag{4.6}$$

with

$$\delta Q_{0,0} = \sum_X \delta Q^X_{0,0} = \sum_X \sum_{i,j} a^X_{i,j} Q_{i,j} (Q_{0,0} + Q_X) \tag{4.7}$$

where X runs over the four boundaries of pixel $(0,0)$, i.e. $X \in \{(0,1),(1,0),(0,-1),(-1,0)\}$

In order to evaluate the statistical correlations in flat-field exposures introduced by the charge-induced perturbations of drift trajectories, we wish to evaluate

$$Cov(Q'_{i,j}, Q'_{0,0}) = Cov(Q_{i,j}, \delta Q_{0,0}) + [(i,j) \leftrightarrow (0,0)] + O(a^2) \tag{4.8}$$

where $O(a^2)$ stands for expressions quadratic in the $a^X_{i,j}$ coefficients of expression 4.7. We will stick to first order perturbation expressions, as real data indicates that this is justified. In the case

where the pixel (i,j) is not a nearest neighbor of $(0,0)$, we have:

$$\begin{aligned} Cov(Q_{i,j}, \delta Q_{0,0}) &= Cov\left(Q_{i,j}\ ,\ \sum_{k,l} a^X_{k,l} Q_{k,l}(Q_{0,0}+Q_X)\right) \\ &= Var[Q_{i,j}] \sum_X a^X_{i,j} E[Q_X + Q_{0,0}] \end{aligned} \tag{4.9}$$

where E stands for the expectation value. For a flat-field illumination of average content μ and variance V, the above expression reads:

$$Cov(Q_{i,j}, \delta Q_{0,0}) = 2\mu V \sum_X a^X_{i,j} \tag{4.10}$$

In case the pixel (i,j) is a nearest neighbor of pixel $(0,0)$, say Y, we have two terms in the covariance:

$$\begin{aligned} Cov(Q_Y, \delta Q_{0,0}) &= Cov\left(Q_Y, \sum_X \sum_{i,j} a^X_{i,j} Q_{i,j}(Q_{0,0}+Q_X)\right) \\ &= Var[Q_Y]\left[\sum_{X\neq Y} a^X_Y E[Q_{0,0}+Q_X] + \sum_{(i,j)\neq Y} a^Y_{i,j} E[Q_{ij}]\right] \\ &\quad + a^Y_Y Cov(Q_Y, Q_Y(Q_{0,0}+Q_Y)) \end{aligned} \tag{4.11}$$

We have:

$$\begin{aligned} Cov(Q_Y, Q_Y(Q_{0,0}+Q_Y)) &= \mu Cov(Q_Y, Q_Y) + Cov(Q_Y, Q_Y^2) \\ &= \mu V + Cov(Q_Y, Q_Y^2) \end{aligned}$$

If Q_Y follows a probablity density function symmetric around its mean, we have

$$Cov(Q_Y, Q_Y^2) = 2\mu V$$

For a Poisson distribution, this becomes $Cov(Q_Y, Q_Y^2) = 2\mu^2 + \mu$ where the second term is the skewness contribution, negligible for actual flat-fields.

In the context of a flat-field, the three terms of 4.11 become:

$$Cov(Q_Y, \delta Q_{0,0}) = \mu V \left[2\sum_{X\neq Y} a^X_Y + \sum_{(i,j)\neq Y} a^Y_{i,j}\right] + 3a^Y_Y \mu V \tag{4.12}$$

Because of the sum rule (eq. 4.4), the second term in [ ] reads $-a^Y_Y$ so that for neareast neighbors, we also have:

$$Cov(Q_Y, \delta Q_{0,0}) = 2V\mu \sum_X a^X_Y \tag{4.13}$$

So whether or not (i,j) is a nearest neighbor, we have for the covariance between pixels in a uniform exposure of average μ and variance V:

$$Cov(Q'_{i,j}, Q'_{0,0}) = 4V\mu \sum_X a^X_{i,j} \tag{4.14}$$

to first order of perturbations. The factor of 4 compared with the factors of 2 in eq. 4.10 and 4.13 comes from the symetric (second) term of eq. 4.8.

It turns out that in order to apply this equation to $(i, j) = (0,0)$, we just have to account for the input "variance":

$$Cov(Q'_{0,0}, Q'_{0,0}) = V + 4V\mu \sum_X a^X_{0,0} \tag{4.15}$$

where in practice, the $a^X_{0,0}$ are negative and are a plausible cause of the photon transfer curve non-linearity.

So, electrostatic influence from collected charge induces covariances between pixels in spatially uniform exposures that scale with both the average and the variance of pixel contents. If one measures correlation coefficients (ratio of covariance to variance), those are expected to scale with the illumination level of the uniform exposure. This is precisely what we observe in figure 2.

With a realistic set of $a^X_{i,j}$ coefficients (e.g. from the simulation 4.1) we observe that the brighter-fatter effect is indeed linear with flux to an excellent approximation (fig 5).

5. Closing the loop: deriving the brighter-fatter slope from flat-field correlations

5.1 Solving for the model coefficients from flat-fields

The first order model described in § 4.2, is entirely specified by the $a^X_{i,j}$ coefficients. Given their symmetries, we only need those for $i, j \geqslant 0$. Furthermore, since these coefficients describe Coulomb forces, they decay with distance, and we can neglect those describing large distance interactions. If we restrict ourselves to $0 \leqslant i, j \leqslant n$, we have a priori $4(n+1)^2$ coefficients to determine. However, each boundary is shared by two pixels and charge conservation reduces the number of coefficients by roughly a factor of 2, more precisely to $(n+1)(2n+4)$. From the flat-fields, we only have $(n+1)^2$ correlations to measure, which is short by about a factor of 2.

In order to solve anyway, we have imposed ratios of coefficients addressing similar source-test separations, using some reasonable approximation for the dependence of electric fields on distance. Once we have solved, we can evaluate the brighter-fatter slope by scaling up faint spots or stars, and "scrambling" them using eq. 4.7. We have checked that the resulting brighter-fatter slope is reasonably independent of the chosen parametrization of distance dependence of the electric field.

5.2 Comparing predicted and measured brighter-fatter slopes

The comparison between the brighter-fatter slopes predicted from flat-fields and the ones measured directly is done using the same data used for the detection of the brighter-fatter effect. As just mentioned, we transform faint spots or stars into bright ones by scaling them up and transforming the image using eq. 4.7. In order to account for the small amount of broadening already present in faint spots or stars, we first apply the reverse transformation of eq. 4.7 to faint spots, which we approximate by the same expression with opposite a coefficients. We have checked that for the typical size of the a coefficients, flipping signs is a fair approximation of the inverse transformation[3], especially for faint stars.

[3]Typically, a star with 100 ke at peak that sees it size increase by $\sim$2%, is decreased by the flipped transformation to its original size at the per mil level. So, for bright stars, applying successively the regular and flipped transformations causes size changes that differ by $\sim$5%.

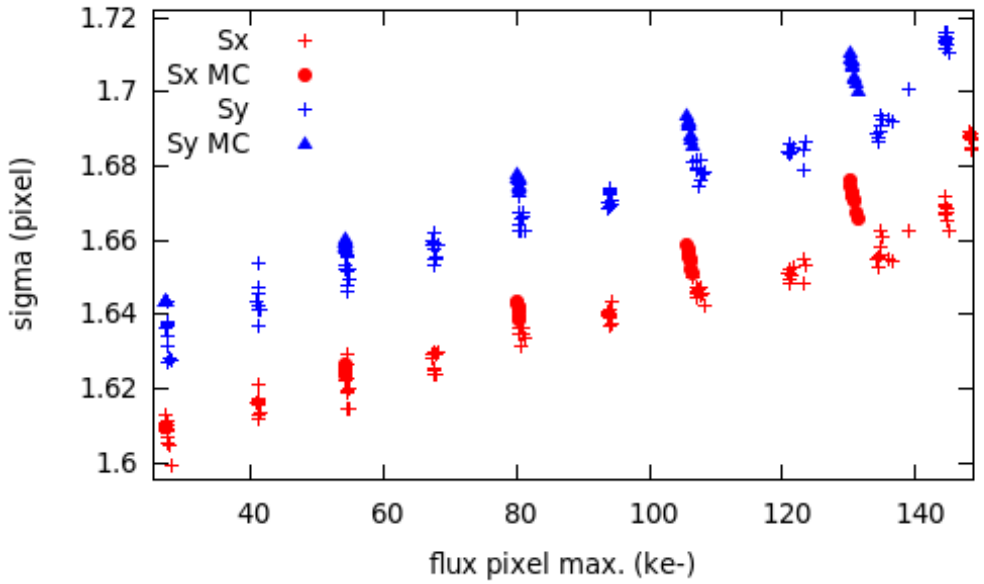

Figure 6. Comparison of sizes of real spots (Sx, Sy) with sizes of scrambled spots (Sx MC, Sy MC), as a function of their peak flux. "MC" stands for a Monte Carlo propagation of shot noise affecting correlation measurements in flat-fields. The predicted brighter-fatter slopes are larger than the measured ones for both x and y directions, for this data sample collected at 550 nm. The 900 nm data set displays very similar trends.

For the E2V CCD250, we compare the measured sizes of real spots and scrambled spots in fig. 6: the brighter-fatter slopes are similar at the $\sim$20% level, where only a fraction of the difference can be attributed to the shot noise affecting the measurements of correlations. Indeed, the trend is very similar on the independent data set taken at 900 nm.

We display a similar comparison for a selected DECam CCD in fig. 7. The disagreement of slopes is of about the same size, but exhibits the opposite sign, and might be affected by the overall non-linearity of response (that we briefly discuss in § 6). The precision is limited by statistics of the star measurements. We have measured the brighter-fatter slopes for all chips of the mosaic and find an rms of the distribution about two times larger than expected from propagating the shape measurement noise. We hence do not conclude yet that brighter-fatter slopes are compatible on different chips of the mosaic. We can however compare the average measured brighter-fatter slope to the average one predicted from correlations, and find the prediction from flat-fields to be $\sim$20% larger than the direct measurement.

We have finally carried out the same comparison for Megacam sensors. We have taken the star size measurements from Tab. 4 of [3], and the brighter-fatter slope predicted from flat-fields correlations is $\sim$30% smaller than these measurements. However, the comparison is here limited by the small amount of flat-field data we have been able to use, and by the fact the brighter-fatter effect is small (less than 0.5% over the full scale) and somehow "hidden" by more trivial variations of the object's sizes with color, coupled to flux-color trends in the star sample.

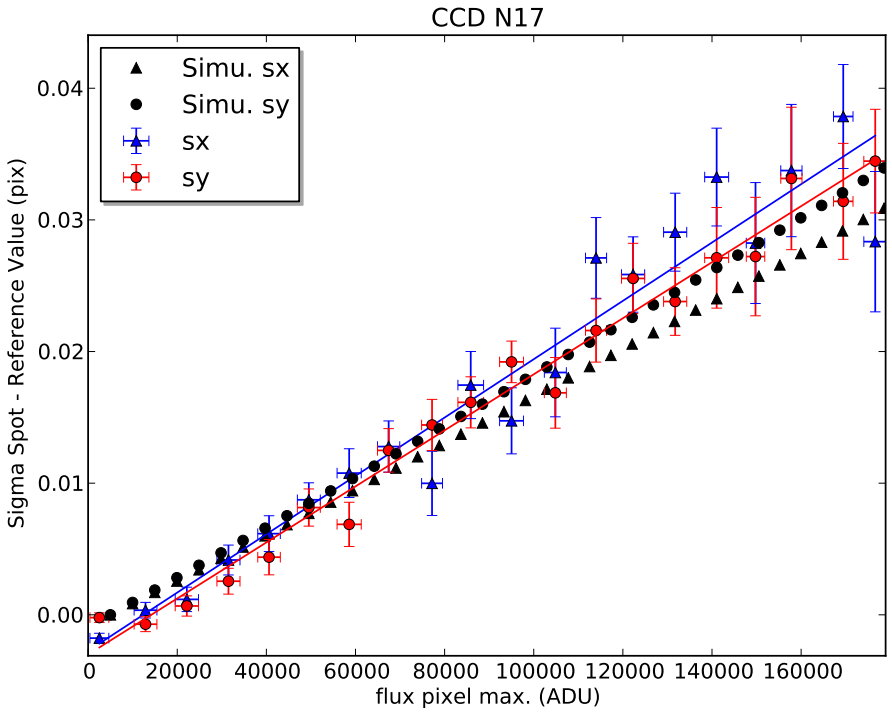

Figure 7. Comparison of sizes of real stars, and the evolution of the scrambled PSF model (modeled as independent of flux) for CCD 17 of DECam. We have subtracted the image quality of the image from each star measurement, which is on average $\sigma_{IQ} \simeq 1.7$ for this data sample, i.e the image quality is $\sim$4 pixels FWHM. The agreement is fair, but statistically limited by the number of stars we measured. When averaging over CCDs (see text), the slopes disagree by $\sim$20%.

6. Discussion

Coulomb forces within CCDs are a plausible cause of the brighter-fatter effect and statistical correlations observed in flat-fields. The latter are also related to the flattening of the PTC commonly observed with CCD devices. We propose a scheme to describe the brighter-fatter effect at the pixel level using measured correlations in flat-fields that matches measurements at a typically $\sim$20% accuracy.

Further work is required before we can practically handle the brighter-fatter effect along this proposed line. We have neglected the fact that charges in the CCD not only alter drift lines but also reduce the longitudinal drift field (this is usually referred to as "space charge effect"). As a result, the measured correlations in flat-fields are slightly increased by the effect, generally absent in science data because the sky level is most often deliberately kept low by adjusting the exposure time. This decrease of the longitudinal drift field also slightly increases the lateral diffusion for bright spots with respect to faint ones (see the contribution by S. Holland at this workshop). However, the size of this effect is much smaller than what we observe, in particular for the practical case of a PSF broader than 3 pixels FWHM. Among the three sensor types we have discussed, the one from DECam is the most affected by these space-charge effects because it has the lowest nominal drift

field: the bias voltage is 40 V for a thickness of 250 μm.

Properly handling the brighter-fatter effect aims at evaluating the PSF shape at all fluxes where it is practically needed. The non-linearity of response of the sensor (typically due to the electronic chain) can also produce variations of the PSF size with flux, and has to be handled separately. In our comparisons, we have ignored possible non-linearities. For Megacam, there is practical evidence that they are very small (see Appendix C in [5]). For the E2V CCD data, variations of the light source intensity with time limit our capability to address linearity. For DECam, a significant non-linearity has been detected (see the contribution of G. Bernstein at this workshop) by regressing the average measured level of dome flat-fields against exposure time. One might wonder if the electronic chain responds in a similar way to high steady fluxes (as for high-level flat-fields) and to localized high signal levels in a few pixels (as for bright stars). Taking these non-linearity measurements at face value increases the observed non-linearity but the disagreement between measured and simulated bright-fatter slopes remains of similar size, with the opposite sign.

One obvious weakness of the proposed approach is that the general model has more coefficients than the number of two-point flat-field correlations we can measure. One possible way out is to improve electrostatic simulations in order to derive relations between model coefficients which are reasonably independent of the unknowns affecting the sensor layout. Regarding measurements, we have not settled yet if higher order flat-field correlations deliver new information compared with two-point correlations, nor if higher order correlations are practically measurable. One can also consider measuring the response of sensors to other patterns than just flat-fields to constrain the evolution of shapes of sharp spots. How the brighter-fatter effect varies with image quality likely contains some amount of information.

Regarding the practical handling of the brighter-fatter effect in reduction pipelines, we can already imagine two avenues: the simple one consists in "de-scrambling" the images at the pixel level, using some inverse of relation 4.7. If just flipping signs of the a coefficients is not accurate enough, some refinement can easily be devised. However, this model assumes that the image is properly sampled, i.e. that the flux on pixel boundaries is well approximated by interpolating between the pixel contents. This is likely to be an unacceptable approximation for sharp images as typically obtained from space. One can then account for the brighter-fatter effect inside the PSF model, using the PSF itself to evaluate the charge density along pixel boundaries.

It is likely that the crude technique we have exposed in this work can handle the brighter-fatter effect at the $\sim$10% accuracy, with some refinements, possibly along the lines mentioned in the above paragraphs. It is certainly premature to consider that a 1% accuracy is within reach. In particular, the brighter-fatter effect is anisotropic, because the pixel boundaries separating line and rows of CCDs are generated via totally different mechanisms for most CCD types. We believe that the way to account for the evolution of PSF ellipticity with flux at the $\sim 10^{-4}$ level, as required for very large scale weak shear programs (see [2]), is still an open question.

Acknowledgments

We thank the organizers of the workshop for inviting us to participate. Before and after the workshop, we had fruitful exchanges with R. Lupton. We used freely available science verification

DECam data. We had several useful discussion with members of the DES collaboration, in particular D. Tucker and G. Bernstein who are in close contact with the data, and J. Estrada for his deep knowledge of the DECam sensors. DECam non-linearity of response was derived by H. Lin. We used Megacam science data from the CFHTLS, now freely available. The Megacam flat-field raw was made available to us by J.-C. Cuillandre.

References

[1] M. Downing, B. Baade, P. Sinclaire, S. Deiries, and F. Christen, *CCD riddle: a) signal vs time: linear; b) signal vs variance: non-linear*, *Proc SPIE* (2006) 6276–09.

[2] R. Laureijs, J. Amiaux, S. Arduini, J. . Augueres, J. Brinchmann, R. Cole, M. Cropper, C. Dabin, L. Duvet, A. Ealet, and et al., *Euclid Definition Study Report*, *ArXiv e-prints* (Oct., 2011) [arXiv:1110.3193].

[3] P. Astier, P. El Hage, J. Guy, D. Hardin, M. Betoule, S. Fabbro, N. Fourmanoit, R. Pain, and N. Regnault, *Photometry of supernovae in an image series: methods and application to the SuperNova Legacy Survey (SNLS)*, A&A **557** (Sept., 2013) A55, [arXiv:1306.5153].

[4] É. Durand, *Électrostatique*. No. vol. 3. Masson, 1964.

[5] N. Regnault, A. Conley, J. Guy, M. Sullivan, J. Cuillandre, P. Astier, C. Balland, S. Basa, R. G. Carlberg, D. Fouchez, D. Hardin, I. M. Hook, D. A. Howell, R. Pain, K. Perrett, and C. J. Pritchet, *Photometric calibration of the Supernova Legacy Survey fields*, A&A **506** (Nov., 2009) 999–1042, [arXiv:0908.3808].